# TIME AND FREQUENCY TRANSFER COMBINING GLONASS AND GPS DATA

**Pascale Defraigne[1], Quentin Baire[1], and A. Harmegnies[2]**
**[1]Royal Observatory of Belgium (ROB)**
**Avenue Circulaire, 3, B-1180 Brussels**
**E-mail: *p.defraigne@oma.be, q.baire@oma.be***

**[2]Bureau International des Poids et Mesures**
**Pavillon de Breteuil,**
**92312 Sèvres, France**
**E-mail : *aharmeg@bipm.org***

**Abstract**

***Measurements from Global Navigation Satellite Systems (GNSS) have been used since the eighties to perform precise and accurate Time and Frequency Transfer (TFT). Two main approaches are used presently: the Common View or All in View based on the Common GPS GLONASS Time Transfer Standard (CGGTTS) and the Precise Point Positioning (PPP). Concerning the CGGTTS approach, in order to allow the use of GLONASS data from geodetic-type receivers providing only raw data in RINEX format, the R2CGGTTS software developed initially for GPS at the Royal Observatory of Belgium (ROB) was updated. The GLONASS navigation files are used for the determination of satellite clocks and positions, and the computation procedure to get the CGGTTS data from the pseudorange measurements is applied similarly as for the GPS satellites. In parallel, we also upgraded the PPP software Atomium developed at the ROB to allow the use of the Russian GLONASS constellation. The clock solution is then obtained through the analysis of dual-frequency carrier-phase and pseudorange measurements. This study combines GPS and GLONASS observations in PPP in order to determine the added value of the GLONASS data in geodetic time transfer.***

## INTRODUCTION

Measurements from Global Navigation Satellite Systems (GNSS) have been used since the eighties **[1]** to perform precise and accurate Time and Frequency Transfer (TFT). In its classical version, the GPS time transfer is performed using clock offsets collected in a fixed format, called CGGTTS (Common GPS GLONASS Time Transfer Standard), as described in **[2,3]**. These clock offsets are obtained from the pseudorange measurements, corrected for the signal travel time (satellite-station), for the troposphere and ionosphere delays, and for the relativistic effects. A smoothing is then performed over 13 minutes observation tracks. Starting with C/A code receivers, the method was then upgraded to take benefit from the dual-frequency receivers measuring codes on both frequencies, which allows one to remove the ionosphere delays at the first order (i.e. 99.9 percent of the effect), thanks to the ionosphere-free dual-frequency combination. This led to a factor of 2 improvement in the precision of the intercontinental time

links (e.g., **[4]**). Some time receivers directly provide the CGGTTS results, but in order to be able to use classical geodetic receivers driven by an external clock for the time transfer applications with the same standards, dedicated software named R2CGGTTS was produced to compute the CGGTTS files from the raw observation data provided by the receivers in the RINEX format **[5]**. This software is presently used by a large portion of the time laboratories for their participation to TAI, through the technique TAIP3 **[6]**. Thanks to the growing constellation of GLONASS, some time laboratories have now upgraded their equipment with receivers capable of observing both GPS and GLONASS. We, therefore, adapted the R2CGGTTS software to the use of GLONASS observations, as will be explained in the first part of the paper.

A more precise version of GNSS TFT consists of using both code and carrier-phase observations. The use of PPP, i.e. Precise Point Positioning **[7]**, for time and frequency transfer has been extensively studied and developed in the last few years **[**e.g., **8-11]**. Presently several time links in TAI are based on PPP solutions **[12]**. Only GPS measurements are currently used, while the method should find a significant improvement from the combined use of additional constellations, such as GLONASS, Galileo, and COMPASS, thanks to the increased number of satellites and signals. This paper proposes a first step in this evolution with the combination of GPS and GLONASS data. This is now possible thanks to the effort of the IGS during the last decade to use the GLONASS data for positioning and providing therefore precise orbits for the GLONASS satellites consistent with the GPS satellite orbits.

The combination of GPS and GLONASS observations for time and frequency transfer will be done using the Atomium software **[9]**. This software is based on a least-squares analysis of code and carrier-phase GPS measurements, using satellite orbits in the format sp3 and clocks in the RINEX clock format, to determine the receiver clock synchronization error at each observation epoch, a daily position, and the tropospheric zenith path delays each 15 minutes.

A major difference between the GLONASS and GPS constellations is that all the GLONASS satellites do not transmit the same frequency, so that the signal delay in the receiver is different for each satellite group emitting a given frequency. This affects the code measurements, with differential biases up to 25 ns, as already shown by several authors **[13,14]**. These differential biases must be either determined by calibration or estimated in addition to the clock solution.

The paper will study the added value of GLONASS in CGGTTS and PPP. The PPP results were fully presented in **[15]**; we just here provide a summary.

# CGGTTS

As explained in the Introduction, the CGGTTS files contain clock solutions corresponding to the pseudorange measurements, corrected for the signal travel time (satellite-station) based on broadcast satellite orbits, for the troposphere and ionosphere delays, and for the relativistic effects. The final results provided are the midpoint of a linear fit performed over 13-minute observation tracks for each visible satellite. Using dual-frequency observations allows one to remove the first-order ionosphere delay, which will be done here with GLONASS observations.

As the two time scales GPS and GLONASS differ by an integal number of leap seconds (GPS Time = GLONASS Time + leap seconds) and as the observation files are dated in GPS time, while the broadcast navigation message uses GLONASS time as reference, first a correction for system time must be applied. Secondly, while GPS navigation messages provide parameters of keplerian orbits in WGS84 (very close to the ITRF) every 2 hours, the broadcast navigation message of the GLONASS constellation is given as

a set of positions and velocities in the PZ90 Earth-fixed system at a sampling rate of 30 minutes. As we are computing the CGGTTS from RINEX data in post-processing, we have a choice between computing the GLONASS satellite positions either by numerical integration, or by polynomial interpolation. Figure 1 presents a comparison between the CGGTTS results obtained for 1 day with either interpolation or Runge Kutta numerical integration, 4th order. These results have been obtained using the GLONASS pseudoranges from a RINEX observation file provided by the TTS4 receiver located at the BIPM, and connected to an H-maser.

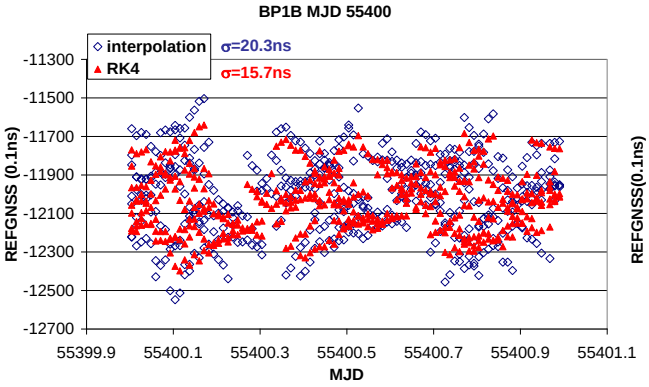


Figure 1. Comparison between the CGGTTS results obtained with either interpolation or Runge Kutta numerical integration, 4th order, for the TTS4 receiver located at the BIPM and connected to an H-maser.

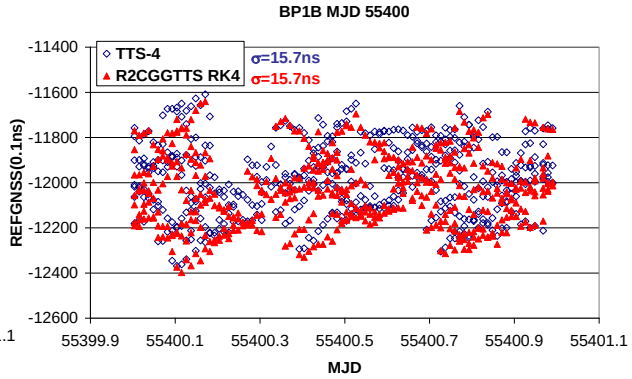


Figure 2. Comparison between the CGGTTS results obtained directly from the TTS4 receiver or using the Rinex2CGGTTS software for GLONASS observations.

As the noise of the results was larger with the linear interpolation, we choose to implement the Runge Kutta integration in the R2CGGTTS software. The results were also validated by a comparison of the CGGTTS data with the TTS4 data, presented in Figure 2. A small bias appears between the two sets of results, probably due to some calibration delay introduced in the TTS4 results but not in the R2CGGTTS results.

Finally, as done by the BIPM for the computation of TAI, we corrected the CGGTTS results computed with broadcast navigation messages by introducing more precise satellite positions and clocks as computed by the ESOC analysis center of the International GNSS Service (IGS). The results so obtained are presented in Figure 3, with a comparison with similar results for the GPS satellites. We can directly observe a larger dispersion of the GLONASS results with respect to the GPS results. This is due to the satellite-dependent hardware delays associated with the satellite-dependent carrier frequencies of the GLONASS constellation, as illustrated in Figure 4. The results of the different satellites are plotted there in different colors. The satellite-dependent biases are clearly visible.

A bias between GPS and GLONASS results is also visible in Figure 3; it is due to the fact that, in the present results, the IGS clock products are used for the GPS satellites, while the ESOC clock products are used for the GLONASS satellites; the reference time scale is, therefore, different.

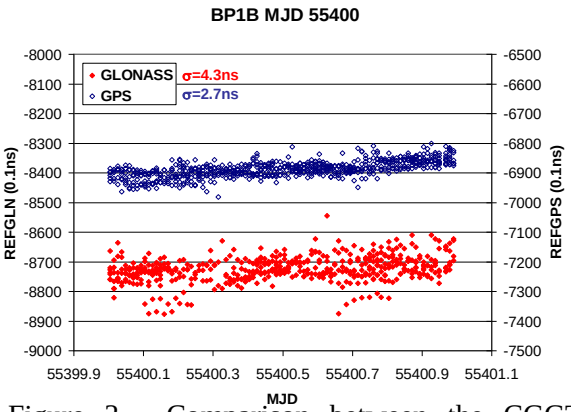


Figure 3. Comparison between the CGGTTS results obtained with either GLONASS satellites or GPS satellites after correction for precise satellite positions and clocks. The ESOC post-processed satellite orbits and clocks are used in both cases.

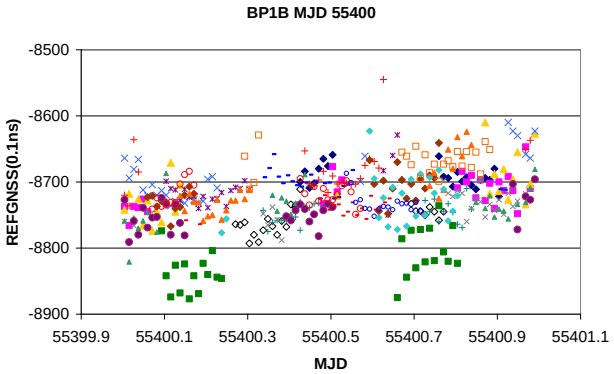


Figure 4. CGGTS results for the different GLONASS satellites, after correction for precise satellite positions and clocks using the ESOC post-processed products.

The CGGTTS results can be used in Common View (CV), or in All in View (AV). The CV means that the time transfer solution at each epoch is a weighted average of the differences between the results obtained in the two stations for a same satellite; the AV means that the time transfer solution at each epoch is the difference between the weighted averages of the different satellite results obtained at this epoch in the two stations. The AV can then be applied on an ensemble of GLONASS and GPS satellites only if the reference time scale of the satellite clocks is the same for the GPS clocks and for the GLONASS clocks. Furthermore, the inter-frequency biases and inter-system biases shown in Figures 3 and 4 must first be removed. These should be either determined numerically or via experimental calibration; a further study will be dedicated to that specific issue.

## PPP USING GPS+GLONASS

In the PPP approach, the measurements of a single station are used to determine the synchronization errors between the clock connected to the receiver and a reference time scale. The latter is the system time scale when using broadcast satellite clock products. When using external satellite clock products as those provided by some analysis center of the International GNSS Service (IGS), the satellite clocks are referred to another time scale. When using the final or rapid IGS products, the reference time scale is the IGS time scale, based on a weighted ensemble of the clocks in the GPS satellites and in the network stations **[16]**.

As for AV, using PPP for time and frequency transfer requires a single common reference for all the satellite clock products used in the analysis. This is not the case with the broadcast satellite clocks: GPS clocks are given with respect to the GPS time and GLONASS clocks are given with respect to GLONASS time. Up to 2008, there existed no reprocessed satellite clock products having the same reference for GLONASS clocks and GPS clocks. Since 2008, the IGS analysis center ESOC has provided combined

GPS and GLONASS products in which the satellite clocks from both constellations are given with respect to the same reference time scale **[17]**. These products will be used here for the combination of GLONASS and GPS in PPP.

The ionosphere-free combinations of measurements taken in a given station *r* from a GNSS satellite *s* can be modeled as

$$L_3{}^{r}{}_{s} = R^{r}{}_{s} + c(-\tau_r + \tau^{s} + trop_r{}^{s}) + N_3{}^{r}{}_{s}(\lambda_3 + w_r{}^{r}{}_{s} + \varepsilon_L r^{r}{}_{s} \quad (1)$$

for the carrier-phase measurement, and

$$P_3{}^{r}{}_{s} = R^{r}{}_{s} + c(-\tau_r + \tau^{s} + trop_r{}^{s}) + \tau_d(n) + \varepsilon_{Pr}{}^{s} \quad (2)$$

for the pseudorange measurement, with $R$ the geometric distance receiver-satellite, $\tau^s$ and $\tau_r$ the satellite and station clock errors, $trop_r^s$ the tropospheric delay, $\lambda_3$ the carrier-phase wavelength for the ionosphere-free combination, $N$ the phase ambiguity (float in this case), $w$ the phase windup, $\varepsilon$ the noise, and $\tau_d(n)$ the uncalibrated receiver hardware delay corresponding to the ionosphere-free combination for the frequency channel $n$, which is constant for all GPS code measurements, but not for GLONASS, as carrier frequencies depend on the emitting channel. The parameters $\tau_d(n)$ can be either estimated through receiver calibration, and, hence, introduced in the analysis as fixed values, or estimated as an additional set of unknowns. There are presently no calibration values available for the existing dual-frequency GLONASS receivers so that only the second alternative can be used. The satellite hardware delays, depending on the frequency channel too, but also on the satellite architecture, are included in the satellite clock products and, therefore, do not require to be modeled in our analysis.

For this study, we have used the software Atomium **[9]**, developed at the Royal Observatory of Belgium (ROB) for GNSS processing. In the PPP analysis, the observation equations (1) and (2) are solved via a least-squares analysis, to determine the station position, the wet tropospheric zenith path delay every 15 minutes **[18]**, and the clock synchronization error between the station clock and the reference time scale of the satellite clock data. In addition, when combining GPS and GLONASS data, the estimation of the uncalibrated receiver hardware delays for the GLONASS frequencies has been added in the least-squares inversion, as biases with respect to the clock solution provided by GPS pseudoranges. These biases are considered as a constant for each day analyzed.

A set of three GPS+GLONASS IGS stations with a stable external frequency was chosen for this analysis. They were used to form different time links: a medium baseline (ONSA-MAR6, 470 km) and a long baseline (ONSA-WTZR, 920 km). The time transfer solutions have been computed for a period of 5 days in September 2009 and a period of 4 days in January 2010 to illustrate the behavior of the solution in the case of a tracking interruption, which appeared in WTZR during the MJD 55255.

We also tested the sensitivity of the solution to the estimation of the frequency-dependent biases of the GLONASS pseudoranges. To that aim, we used in addition to GPS data either GLONASS code and carrier-phase data, or only carrier-phase GLONASS data, in which case no differential biases must be estimated.

# PPP COMBINING GPS AND GLONASS CODE AND PHASES MEASUREMENTS

Using the ESOC products for GPS and GLONASS satellite orbits and clocks, we combine here GPS and GLONASS data in a PPP analysis. The differences of the PPP clock solutions obtained with and without the GLONASS data during 5 days are presented in Figure 5 for the IGS stations MAR6, ONSA, and WTZR. These differences are lower than 200 ps peak to peak. The differences were also computed over a 6-week period for the station WTZR, and the same conclusion was drawn concerning the magnitude of the differences.

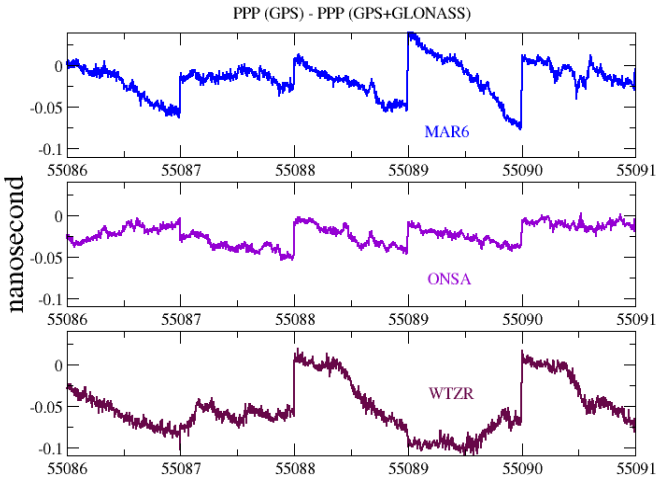


Figure 5. Differences between the PPP clock solutions obtained with GPS data only or using bot GPS and GLONASS data.

In order to validate the PPP clock solutions so obtained, and to compare them with the IGS combined solutions, it is necessary to use baselines. Indeed, the reference time scale of the ESOC satellite clocks is one station clock of the network used for the ESOC orbit computation, while it is the IGS time scale for the IGS clock products. The clock solution obtained from a PPP analysis is, therefore, the clock synchronization error with respect to the ESOC reference when ESOC products are used, and with respect to the IGST when the IGS combined solutions are used. The difference between two PPP clock solutions obtained with the ESOC products gives then a time link that can be compared to the same time link obtained from the difference between IGS station clock solutions.

Figure 6 shows the differences between the PPP solutions and the IGS solutions for three links based on the same stations as before. We can observe that adding GLONASS data to the PPP processing modifies some intra-day variations of the PPP solutions and, in particular, the daily drifts with respect to the IGS solutions. The estimated position of all three stations computed with GPS+GLONASS are close to the estimated position computed with GPS-only: the differences between both are at the level of 2-3 mm in each direction. This position change can explain partly the change of slope of the clock solution when adding GLONASS to GPS measurements in the PPP computation, as shown in **[9]**.

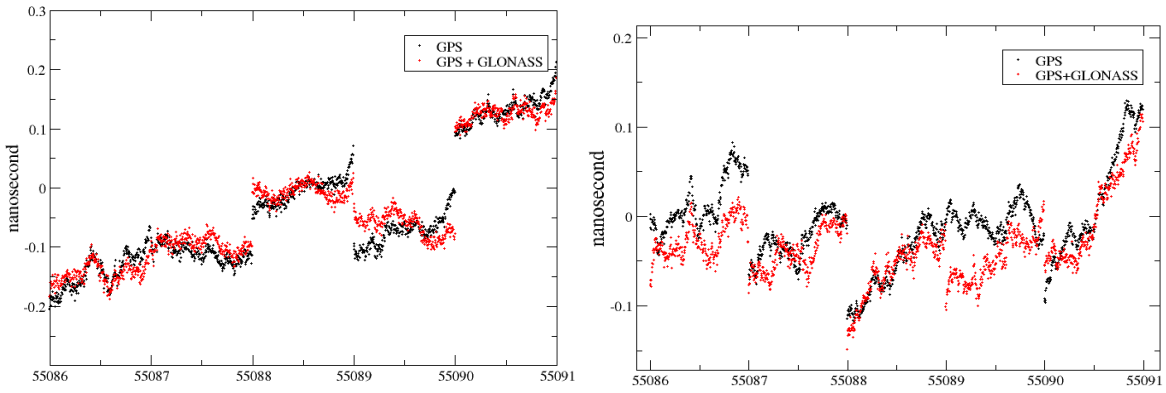


Figure 6. Differences between the Atomium PPP solution and the IGS solution for the time links ONSA-MAR6 (left) and ONSA-WTZR (right).

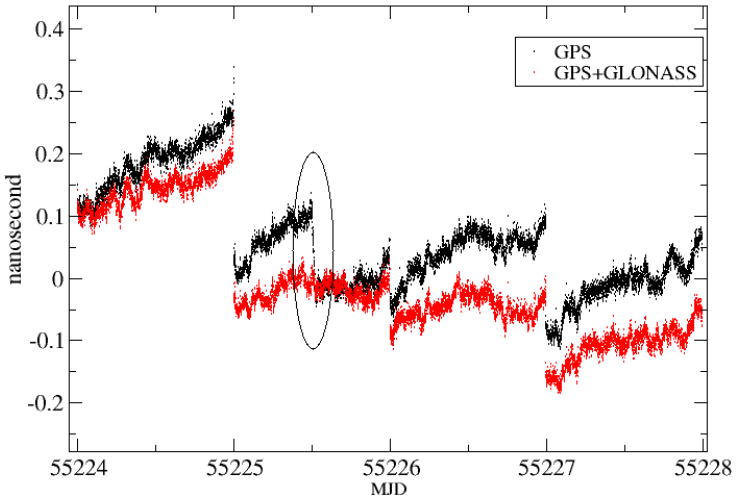


Figure 7. Differences between the Atomium PPP solution and the IGS solution for the time link ONSA-WTZR, with a tracking interruption in WTZR during the MJD 55225.

The link ONSA-WTZR was also computed for a second time span, during which we observed a tracking interruption in WTZR (Figure 7). This creates a data gap in the WTZR observations, which forces the Atomium software to estimate different ambiguities before and after the gap, using approximately two times fewer pseudorange data in each part. There is no jump in the IGS solution at that epoch, as the IGS solution uses the integer ambiguities determined from the double difference network data processing, while Atomium determines floating ambiguities in the least-squares inversion. This jump of 200 ps disappears when adding GLONASS code and phase measurements to GPS data within the analysis, thanks to the increased number of data, which favors a better determination of the ambiguities in both parts, before and after the data gap in WTZR.

# PPP COMBINING GPS WITH ONLY GLONASS PHASES

This section investigates the sensitivity of the solution to the determination of the differential biases for GLONASS frequency channels. The need to determine these 12 additional unknowns can affect the least-squares adjustment and, hence, the clock solution, and an erroneous estimation of some biases could also degrade the solution. We, therefore, combined the GPS code and phase measurements with GLONASS carrier-phase measurements. It allows us to combine GPS and GLONASS data, using the GLONASS carrier-phase observations as additional data for the determination of the clock syntonization errors (i.e. frequency transfer), without adding new parameters to be estimated.

The ambiguities of the GLONASS satellites are in that case estimated with respect to the GPS code measurements.

Figures 8 and 9 present the comparison between the PPP Atomium solutions using either GPS and GLONASS full data or GPS full data with only GLONASS carrier-phase data for the three solutions investigated before. For the two solutions based on continuous observations (Figure 8), the differences are always below 50 ps, i.e. at the present level of precision of PPP software as announced in **[12]**. However, we now retrieve a jump in the link ONSA-WTZR for the period containing a data gap in the observations of WTZR (Figure 9, blue curve), as for the PPP solution using GPS data only. There is indeed presently no more GLONASS codes helping to calibrate the two parts of the curve. We can, therefore, conclude that the determination of the inter-frequency biases for the GLONASS code data does not deteriorate the solution, and even helps to determine the ambiguities so that both GLONASS code and carrier phases should be used when combining this constellation with GPS for TFT applications.

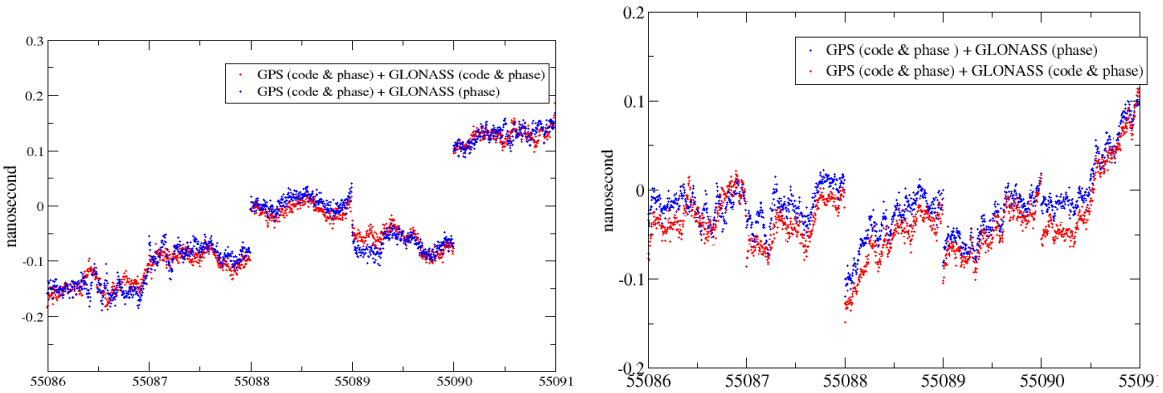


Figure 8. Differences between the Atomium PPP solution and the IGS solution for the time links ONSA-MAR6 (left) and ONSA-WTZR (right); combined analysis of GPS and GLONASS data using or not the GLONASS codes.

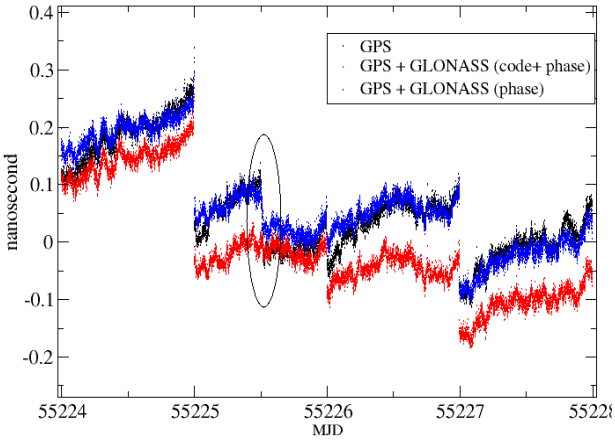


Figure 9. Differences between the Atomium PPP solution and the IGS solution for the time link ONSA-WTZR, with a tracking interruption in WTZR during the MJD 55225; combined analysis of GPS and GLONASS data using or not the GLONASS codes.

## ESTIMATION OF THE HARDWARE DELAYS

In the combined PPP analysis using GLONASS code and carrier phases, the uncalibrated hardware delays are estimated, for each station and each day separately, with the GPS pseudoranges taken as reference. As the ESOC estimates a bias for each receiver-satellite pair, using one receiver-satellite pair as zero reference for each daily data batch **[17]**, the time series of the hardware delays for one station is affected by the change of reference. The time series of the different GLONASS frequency channels is, therefore, presented here for a time link rather than for a station, in order to remove the dependency to the unknown reference. Figure 10 presents the time evolution of the inter-frequency GLONASS biases determined by the Atomium PPP analysis, for the link ONSA-WTZR for the period from January to November 2009.

The one-sigma uncertainties on these delays range from 100 to 200 ps, depending on the day analyzed. The stability of the differential hardware delays determined in our analysis is channel-dependent; the hardware delays determined are constant over the time, with an RMS between 0.6 and 1.2 ns. As seen in Figure 10, a few small jumps occur for some frequency channels, for which we did not find an explanation. Furthermore, some periodic signal appears between MJDs 54910 and 55030 for channel 4, with a period of 8 days, i.e. the repeat cycle of the GLONASS constellation with respect to the ground. This behavior finds its origin most probably in multipath.

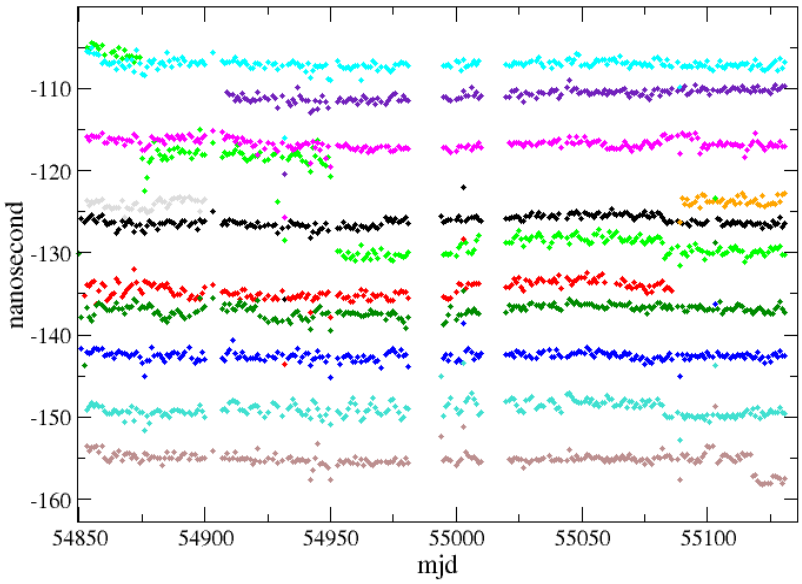


Figure 10. Stability of the different inter-frequency hardware delays determined with respect to the GPS pseudoranges in the PPP

## CONCLUSIONS

This study presented a combination of GPS and GLONASS measurements for time transfer. In a first step, we detailed the upgrade of the R2CGGTTS software in order to be able to use GLONASS observations from RINEX files. The results obtained showed lower noise level when using the Runge Kutta of 4th order than using a polynomial interpolation to get the satellite position from the broadcast navigation files. The results were also validated by a comparison with the CGGTTS results provided by the TTS4 receiver located at BIPM. The results stress the necessity to solve for the inter-satellite biases existing in the GLONASS results due to the satellite-dependent carrier frequencies. When these biases are fixed, GLONASS and GPS data can be combined in Common View as in All in View, but in the latter case, only if the CGGTTS results are corrected for the satellite orbits and clocks using a set of products in which the GPS and GLONASS clocks are given with respect to a same reference, as presently the ESOC products.

In a second step, we studied the addition of GLONASS observations in PPP. The combined GPS+GLONASS PPP was tested using some IGS stations equipped with a multi-constellation receiver connected to an H-maser. Concerning time transfer, i.e. the absolute value of the synchronization errors, also called calibration of the curve, we could find a significant improvement in the case of short data batches. In that case, the calibration of the curve is not well determined when using only GPS data, due to the insufficient number of GPS code data to determine correctly the carrier-phase ambiguities. When adding GLONASS data, the curve retrieves its correct calibration value. This can be important in case of tracking interruption, as was the case in the example presented here. Concerning the frequency transfer with PPP, it was shown that adding GLONASS data modifies the shape of the curve, with a maximum difference of 150 ps peak to peak between the results obtained with and without GLONASS.

The inter-frequency hardware biases for the GLONASS frequency channels were estimated in the least-squares adjustment as one constant value over each day, with a one-sigma uncertainty between 100 and 400 ps. The day-to-day variations of the estimated biases over 200 days were shown to be dependent on

the frequency channel, with a typical repeatability within an RMS of 0.6 ns. In order to test the sensitivity of the combined solution to the determination of these hardware delays, we also combined GPS data (code and carrier phase) with only carrier-phase measurements from GLONASS. The GLONASS ambiguities in that case were determined thanks to the GPS pseudoranges. No improvement was observed in the stability of the solutions. Furthermore, the improvement gained on the calibration of the solution for short data batches, thanks to the GLONASS pseudoranges, was lost. We, therefore, conclude that both code and carrier-phase data from GLONASS should be used when combining this system with GPS for TFT applications.

From this result, it can be concluded that there is no urgent need for receiver absolute calibration of inter-frequency hardware biases, as they can be accurately estimated in parallel to the clock solutions. Moreover, this opens the way to a multi-GNSS time and frequency transfer using as a basis the code measurements from the constellation having the lowest noise and for which the receiver was calibrated. The improved quality of the TFT solutions will be obtained thanks to the accumulation of future GNSS with new satellites such as Galileo, and combined satellite orbit and clock products for the different systems.

## ACKNOWLEDGMENTS

We acknowledge the IGS and ESA/ESOC for making their solutions available.

## REFERENCES

**[1]** D. W. Allan and M. Weiss, 1980, *"Accurate time and frequency transfer during common-view of a GPS satellite,"* in Proceedings of the 34th Annual Frequency Control Symposium, 28-30 May 1980, Philadelphia, Pennsylvania, USA (IEEE), pp. 334-356.

**[2]** D. W. Allan and C. Thomas, 1994, *"Technical directives for standardization of GPS time receiver software,"* **Metrologia, 31,** 69-79, 1994.

**[3]** J. Azoubib and W. Lewandowski, 1998, *"CGGTTS GPS/GLONASS data format Version 02,"* 7th CGGTTS Meeting, 1998.

**[4]** P. Defraigne and G. Petit, 2003, *"Time Transfer to TAI Using Geodetic Receivers,"* **Metrologia, 40,** 184-188.

**[5]** P. Defraigne and G. Petit, 2001, *"Proposal to use geodetic-type receivers for time transfer using the CGGTTS format,"* BIPM Time section Technical Memorandum TM.110.

**[6]** G. Petit and Z. Jiang, 2004, *"Stability and accuracy of GPS P3 time links,"* in Proceedings of the 18th European Frequency and Time Forum (EFTF), 5-7 April 2004, Guilford, England, UK, CD-ROM (file 066.pdf).

**[7]** J. Kouba and P. Heroux, 2001, *"Precise Point Positioning using IGS orbits and clock products,"* **GPS Solutions, 5,** no. 2, 12-28.

**[8]** N. Guyennon, G. Cerretto, P. Tavella, and F. Lahaye, 2009, *"Further characterization of the time transfer capabilities of precise point positioning (PPP): the Sliding Batch Procedure,"* **IEEE Transactions on Ultrasonics, Ferroelectrics, and Frequency Control, UFFC-56,** 1634-41.

**[9]** P. Defraigne, N. Guyennon, and C. Bruyninx, 2007, *"PPP and Phase-Only GPS Frequency transfer,"* in Proceedings of the 2007 IEEE International Frequency Control Symposium Joint with the 21st European Frequency and Time Forum (EFTF), 29 May-1 June 2007, Geneva, Switzerland, pp. 904-909.

**[10]** F. Lahaye and P. Collins, 2009, *"Advances in time and frequency transfer from dual-frequency GPS pseudorange and carrier-phase observations,"* in Proceedings of the 40th Annual Precise Time and Time Interval (PTTI) Systems and Applications Meeting, 1-4 December 2008, Reston, Virginia, USA (U.S. Naval Observatory, Washington, D.C.), pp. 415-431.

**[11]** J. Delporte, F. Mercier, D. Laurichesse, and O. Galy, 2007, *"Fixing integer ambiguities for GPS carrier phase time transfer,"* in Proceedings of the 2007 IEEE International Frequency Control Symposium Joint with the 21st European Frequency and Time Forum (EFTF), 29 May-1 June 2007, Geneva, Switzerland (IEEE), pp. 927-932.

**[12]** G. Petit and Z. Jiang, 2008, *"Precise point positioning for TAI computation,"* **International Journal of Navigation and Observation**, ID 562878, 8 pp.

**[13]** F. Roosbeek, P. Defraigne, and C. Bruyninx, 2001, *"Time transfer experiments using Glonass P-code measurements from RINEX files,"* **GPS Solutions, 5,** No. 2, 51-62.

**[14]** J. Nawrocki, W. Lewandowski, P. Nogas, D. Foks, and D. Lemanski, 2006, *"An Experiment of GPS+GLONASS Common-View Time Transfer Using New Multi-System Receivers,"* in Proceedings of the European Frequency and Time Forum (EFTF), 27-30 March 2006, Braunschweig, Germany (IEEE), pp. 562-565.

**[15]** P. Defraigne and Q. Baire, 2011, *"Combining GPS and GLONASS for Time and Frequency Transfer,"* **Advances in Space Research** (in press).

**[16]** K. Senior, P. Koppang, and J. Ray, 2003, *"Developing an IGS time scale,"* **IEEE Transactions in Ulytrasonics, Ferroelectrics, and Frequency Control, UFFC-50,** 585-593.

**[17]** T. Springer, 2009, *"NAPEOS Mathematical Models and Algorithms,"* DOPS-SYS-TN-0100-OPS-GN, 1.0, 5 November 2009.

**[18]** Q. Baire, P. Defraigne, and E. Pottiaux, 2009, *"Influence of Troposphere in PPP Time Transfer,"* in in Proceedings of 2009 IEEE International Frequency Control Symposium Joint with the 23rd European Frequency and Time Forum (EFTF), 20-24 April 2009, Besançon, France (IEEE), pp. 1065-1068.